Introduction to modeling of laser-produced plasmas

Jiří Limpouch

Czech Technical University in Prague
Faculty of Nuclear Sciences & Physical Engineering
Brehova 7, 115 19 Praha 1, Czechia
jiri.limpouch@fjfi.cvut.cz

Simulation Is an Important Tool in Scientific Research

- Computer simulations are carried out to
  - Understand the consequences of fundamental physical laws
  - Help interpret experiments
    - Can provide detailed information which is difficult to measure
  - Design and predict new experiments

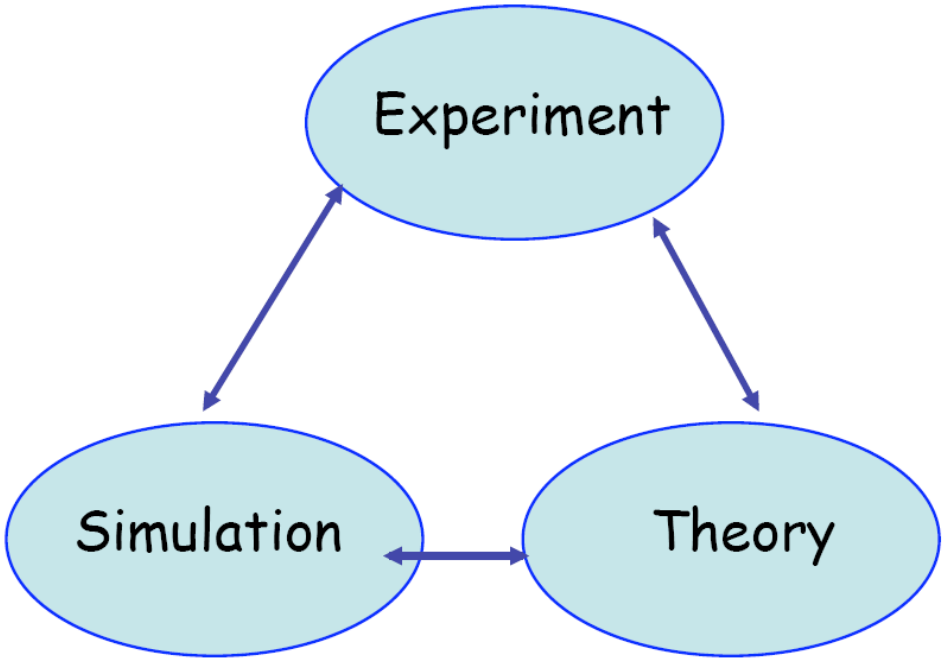

Numerical simulation is not theory!

Approximate theoretical models important, even if analytical solution does not exist

What is numerical simulation?

- The numerical simulation is: writing a program and using the computer to perform a numerical experiment, which can show the time evolution of the nonlinear phenomena.
- **Linear problems:** analytical solutions are available for most linear problems, so numerical simulation is not necessary. *Linear theory provides theoretical basis for validating the simulation results.*
- Unfortunately, most plasma-based systems are highly nonlinear. So the numerical simulation could provide a more solid theoretical basis for studying a highly nonlinear and highly relativistic system.

Numerical simulation methods for LPP

- **Plasma dynamics simulations**
  - Kinetic methods [$\Rightarrow$ distribution function $f(\boldsymbol{r},\boldsymbol{p},t)$]
    - Particle methods
      - Test particle methods
      - Particle-particle methods (small particle number, inefficient)
      - Particle-mesh methods – PIC
      - Mesh-free methods – Tree codes
      - Molecular dynamics methods
    - Solution of equation for distribution function
      - Vlasov equation
      - Fokker-Planck equation (Vlasov-Boltzmann equation)
  - Fluid (hydrodynamic) methods [$\rho(\boldsymbol{r},t)$, $\boldsymbol{u}(\boldsymbol{r},t)$, $T(\boldsymbol{r},t)$]
    - Two-fluid hydrodynamics (rare)
    - One-fluid hydrodynamics (often 2 temperatures, radiation, …)
    - MHD
  - Hybrid methods - part of plasma (e.g. electrons or fast electrons) treated e.g. in kinetic way and part (e.g. ions or ions and thermal electrons) e.g. via fluid methods

Numerical simulation methods (continued)

- **Other simulations**
  - Preprocessors
    - Atomic physics codes – EOS, opacities, atomic physics rates (ionization, recombination, excitation etc)
  - Integrated to plasma dynamics
    - Laser absorption and scattering
    - Calculation of plasma ionization state
    - Radiation generation and radiative transport
    - Nuclear processes
  - Post-processors
    - Simulations of plasma radiation or particle sources
      - Line emission from plasma (including detailed atomic physics)
      - K-α emission (including fast electron transport)
    - Simulation of diagnostics results
      - Synthetic shadowgrams, interferograms, proton deflectometry …

Laser target interactions

- **Laser pulses** (typical) – *nonlinearity parameter* $v_{osc}^2/c^2 \sim I\lambda^2$
  - **nanosecond** – lower laser intensities ($I\lambda^2 \leq 10^{16}$ Wcm$^{-2}\mu$m^2), weaker non-linearities, macroscopic plasma dynamics
  - **femtosecond** – higher laser intensities (relativistic for $I\lambda^2 > 10^{18}$ Wcm$^{-2}\mu$m^2)
- **Targets**
  - **low density** (gaseous) – electron density < critical density, ideal (multiply ionized) plasma
  - **dense targets** (liquid, solid) –
  - in fully ionized solid electron density is 2-3 orders > critical density
  - corona – ideal plasma
  - energy transport–collisional plasma
  - compression region – solid

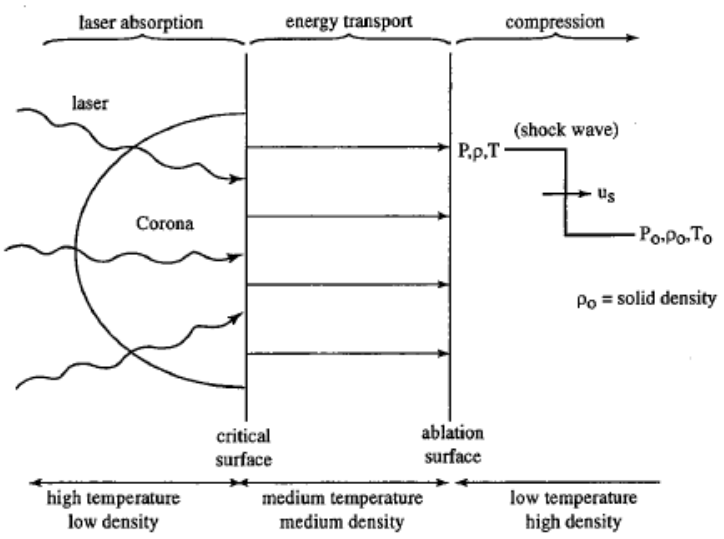

Figure 2.3. A schematic description of laser–plasma interaction.

Plasma dynamics simulations

- **Kinetic versus fluid description**
  - **Kinetic description** is more complete, but it has higher computational demands often imposing limitations (temporal, spatial, etc.)
  - Kinetic models can treat highly nonlinear laser-plasma interaction
  - Kinetic models are usually preferred for high laser intensities and short laser pulses and also for hot plasmas where kinetic effects (e.g. Landau damping) dominate collisional effects
  - Kinetic models are usually limited to **weakly coupled plasma** and they cannot treat global dynamics of laser interaction with bulk dense (solid or liquid) targets
    (Microscopic processes in strongly coupled plasma can be modelled)
  - **Fluid simulations** are preferred for moderate intensities, (sub-) nanosecond laser pulses and **dense targets**, global simulations are feasible (e.g. ICF)
  - Fluid simulations treat non-linear interaction processes only in a phenomenological way, many processes have to be included using analytical models or experience from kinetic simulations

Kinetic plasma models

- ***Particle models versus solving kinetic equations***
  - **Particle models** usually search for distribution function via sampling using macroparticles
  - Particle models are usually *computationally more efficient*
    - Only occupied configuration space is sampled
    - Fundamental physics equations are used
    - Computer codes are usually relatively short
    - Code parallelization is very efficient
  - Additional info is available via *particle tracking*
  - Particle models include some *noise*
  - **Solving kinetic equation** directly is needed if small number of particles (e.g. *energetic tail*) is essential for the studied effect
  - Also *small scale structures* can be resolved (obscured by noise in particle models)
  - Kinetic equation is also solved for processes dominated by collisions (electron thermal transport, collisional absorption)

Simulations methods using particles

- **Particle-particle method**
  - Limitation is the number of arithmetic operations required in the force evaluation scales as N^2
  - Needs special treatment of close encounters
  - Particle-particle approach is proper for small systems with $N<10^6$
- **Particle-mesh method** (Particle-In-Cell)
  - Most popular, very efficient method for weakly-coupled, collisionless or weakly collisional plasmas
  - Especially suited for high-intensity short-pulse lasers
  - Computational mesh is an additional source of noise
- **Particle-cluster methods** (tree-codes, molecular dynamics)
  - Less noisy, but higher computational demands
  - Purely electrostatic interactions are included, induced magnetic field are neglected and no induced electromagnetic waves
  - Used usually for small targets (e.g. clusters) and for studies of microscopic effects

Particle-mesh technique

- Numerical mesh added to more effectively compute the forces acting on model particles.
- Force evaluation based on continuum representation of electromagnetic fields calculated from charge and current densities (**Particle-in-Cell - PIC**)
- The number of floating point operations typically scales as $\alpha N + \beta N_g \ln(N_g) + \gamma N_g$ (N, N_g - number of macroparticles and grid points).

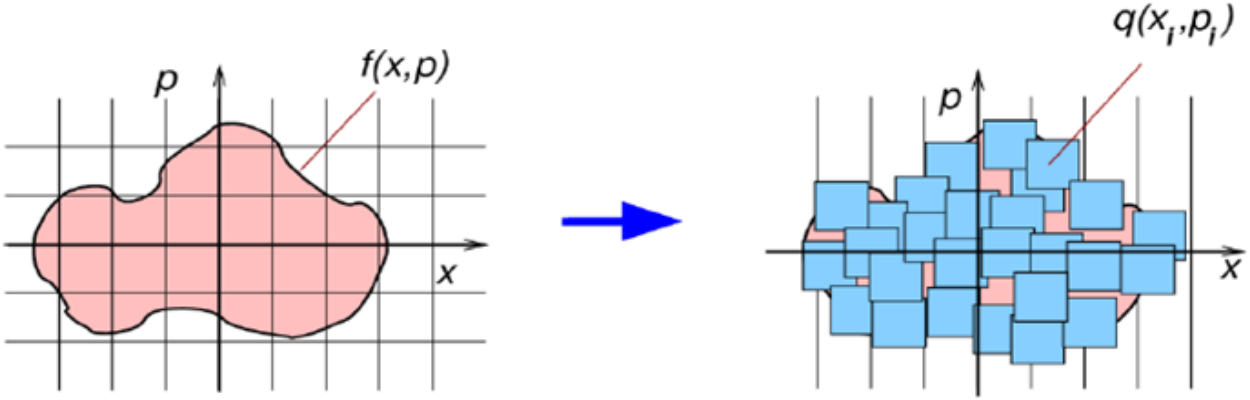

- Kinetic equation solved via sampling
- Macroparticles are clouds of particles (particle dimensions equal to grid cells dimensions, typically comparable to Debye length λ_D)
- Macroparticle has δ function distribution in velocity
- Using mesh practically filters out collisions (strong near binary correlations), thus collisionless Vlasov kinetic equation is solved by PIC codes

Particle-in-Cell code

- The basic cycle of a PIC code

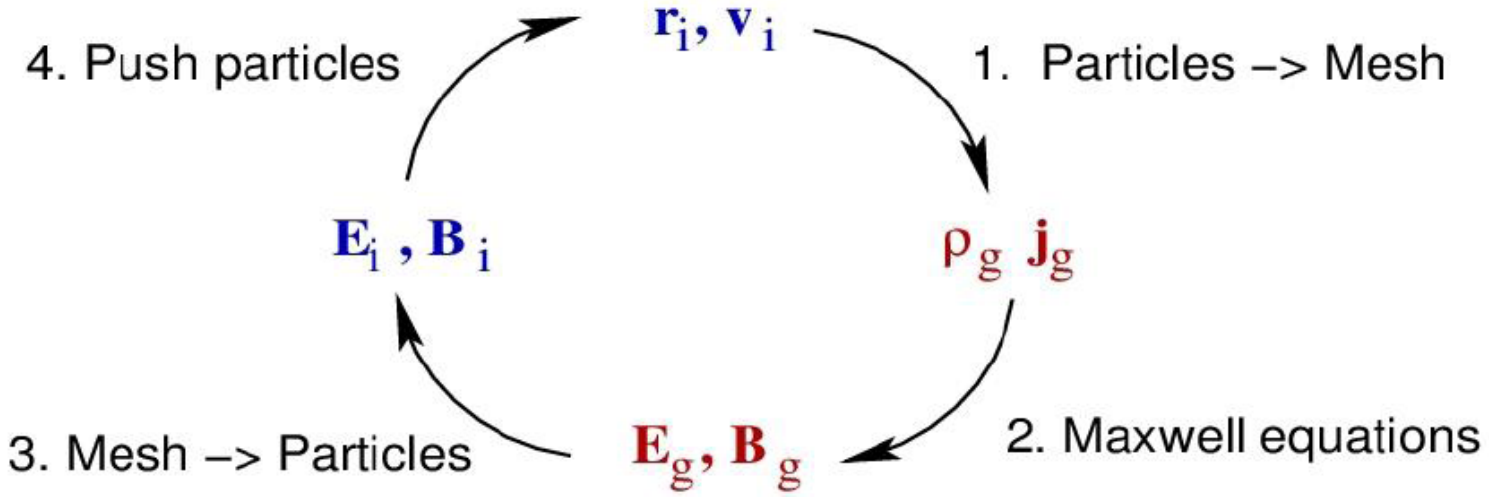

- PIC codes are suitable for uncorrelated (collisionless) or weakly correlated (weakly collisional systems)
- Such systems are dominated by collective modes due to long range Coulomb interaction, the range of wavelengths of these collective modes is bounded at the lower end by the Debye length λ_D due to efficient Landau damping of shorter modes, grid has thus little impact on collective modes
- Most of codes use explicit temporal differencing, the time step thus must be shorter or comparable with inverse plasma frequency ω_p^{-1}.
- Implicit differencing enables longer time step but coding is more difficult.

Categories of PIC models

- **Field components:** Electrostatic, Magnetostatic, Electromagnetic
- **Geometry:** 1/2/3D 1/2/3V, boost frame
- **Equation of motion:** Relativistic or Non-relativistic
- **Boundary conditions:** Absorbing, reflecting or periodic for both particles and fields
- **Binary collisions** may be added (e.g. via Monte Carlo algorithm)

Flow scheme for a typical PIC-MCC code

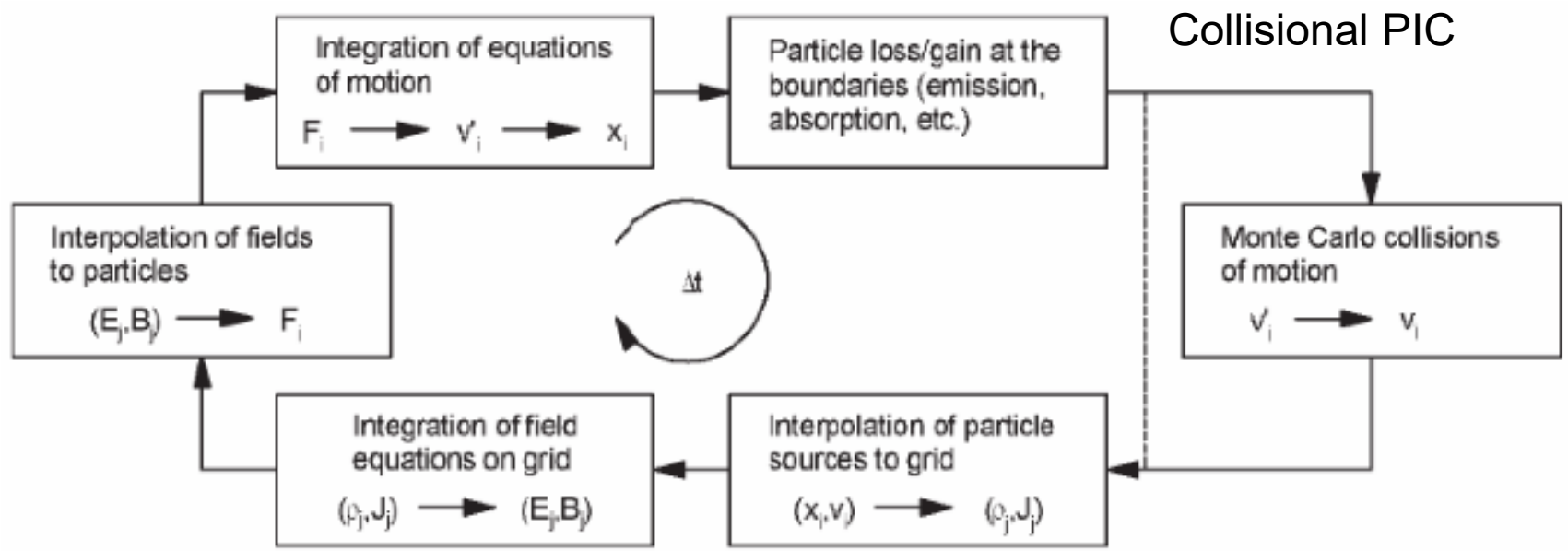

1D3V PIC + 3D time-resolved Monte Carlo simulations

(J. Limpouch *et al.*, LPB **22** (2004), 147–156)

$I = 4\times10^{16}$ W/cm^2, $\theta = 30°$, Al, τ_{FWHM}=120 fs

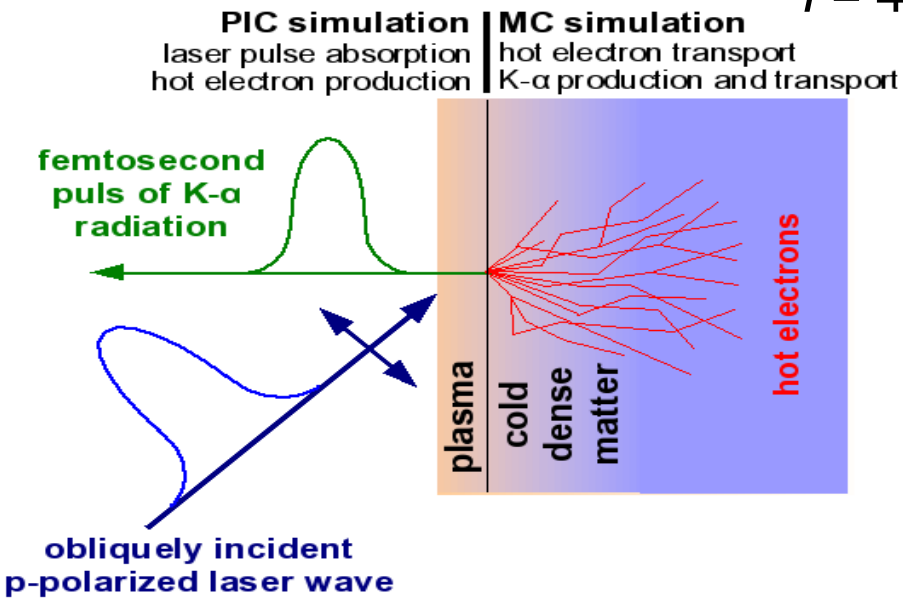

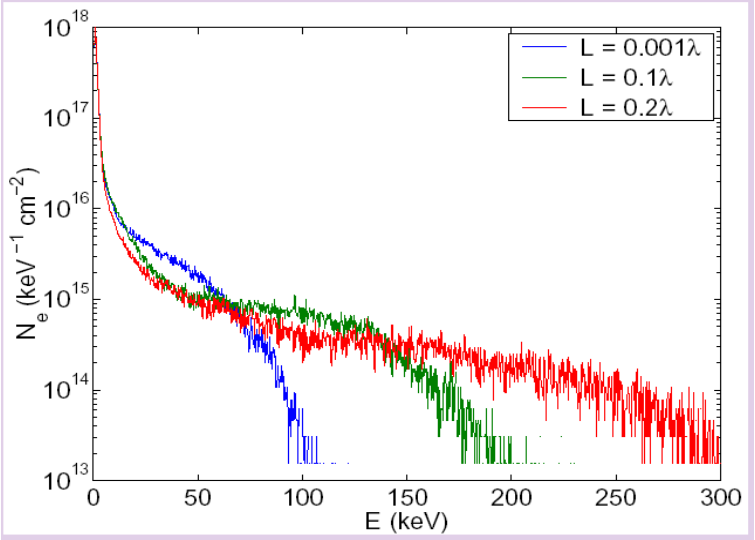

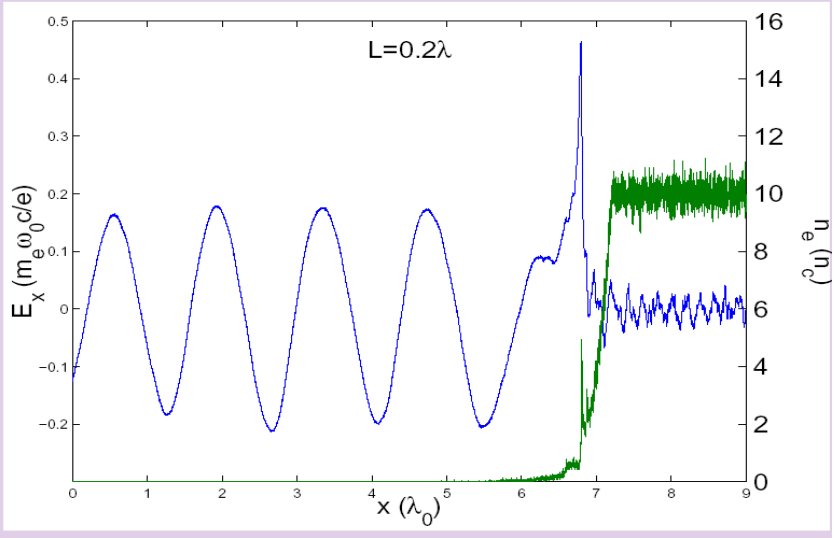

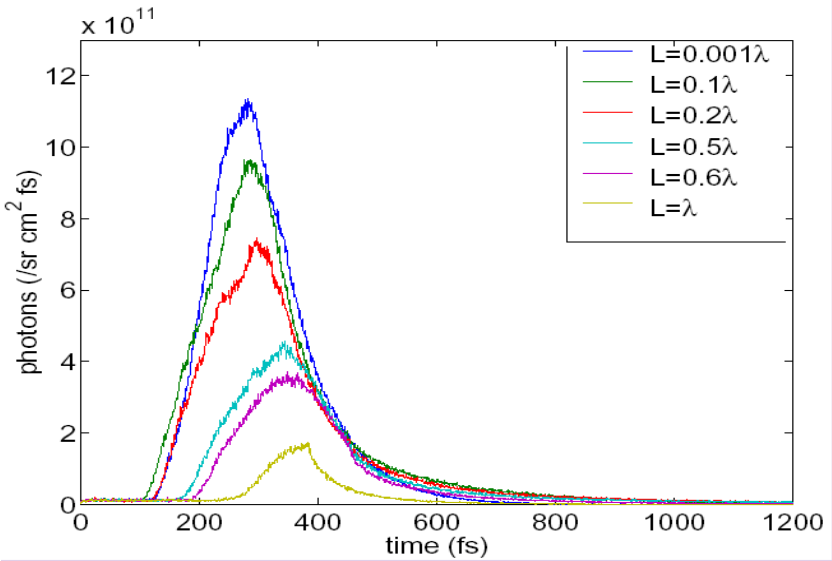

PIC simulations examples

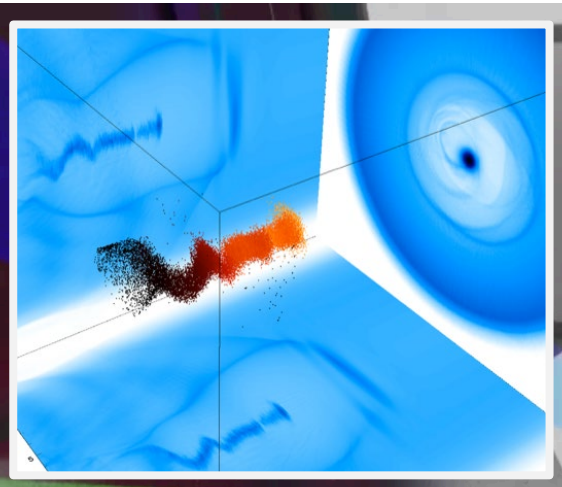

electron beam acceleration

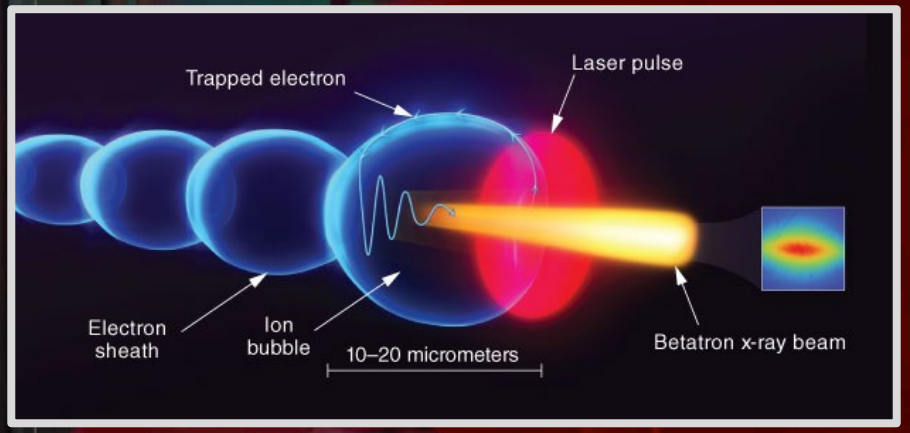

generation of energetic radiation

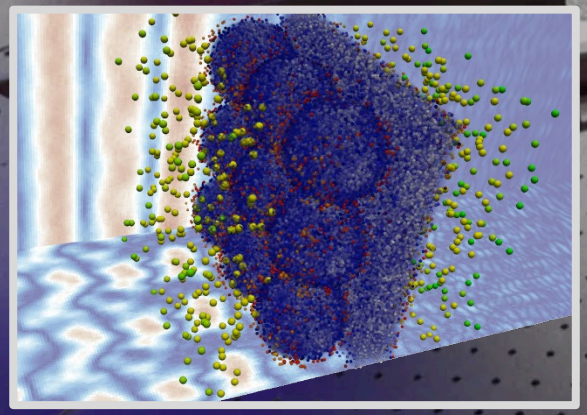

ion beam acceleration

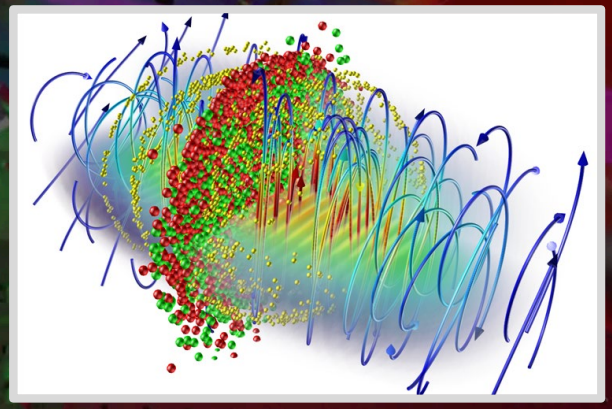

electron-positron pair production

Particle-cluster technique

- **Purely Coulomb interactions** – laser can be included as external field
- The potential of a distant group of particles approximated by low-order multipole expansion.

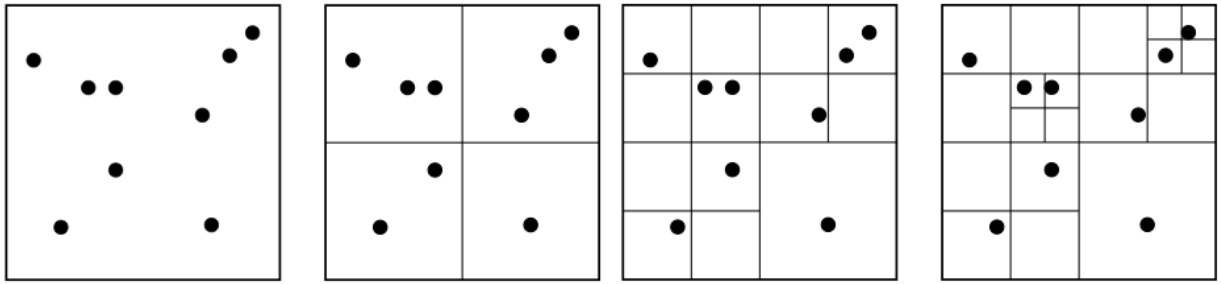

- Various approaches – Molecular dynamics; Tree code
- If periodic boundary conditions are used, Ewald summation can take into account long distance interactions
- Operation count scaling in the force evaluation is below order $N \times \ln(N)$.
- Requires more CPU time than PIC code, but noise is largely suppressed (small-scale features are much better resolved)
- Collisions (strong near binary correlations) can be modelled accurately

Applications of particle-cluster technique

- **Laser-Cluster Interactions**
  - Cluster dimensions smaller than laser wavelength, so only temporal variation of laser field included (macro-particles are used)
  - Open boundary conditions or periodic boundary conditions modelling set of clusters

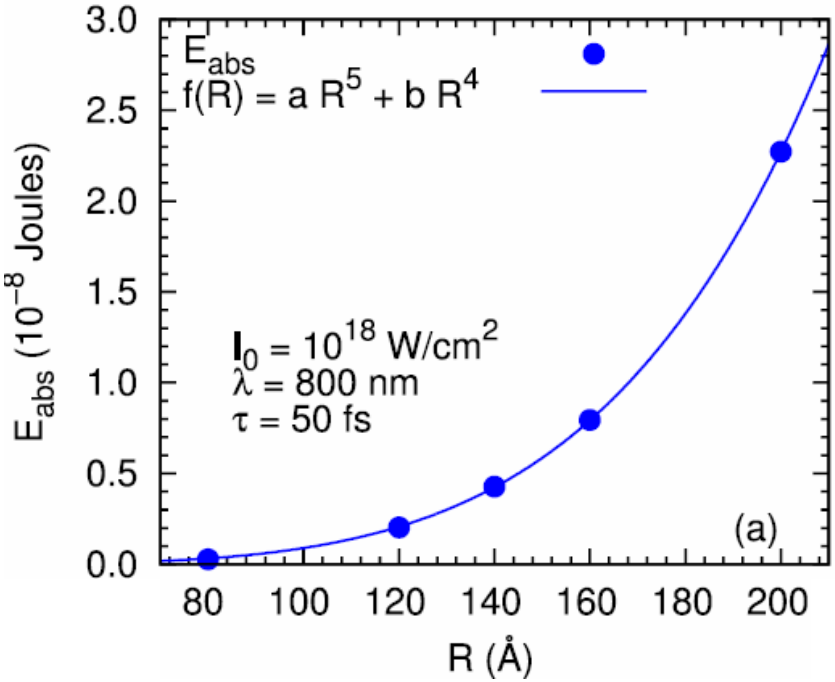

Absorbed laser energy versus D cluster radius. Laser 800 nm, 50 fs, 10^{18} W/cm^2 (Holkundar *et al.*, Phys. Plasmas **21** (2014) 013194)

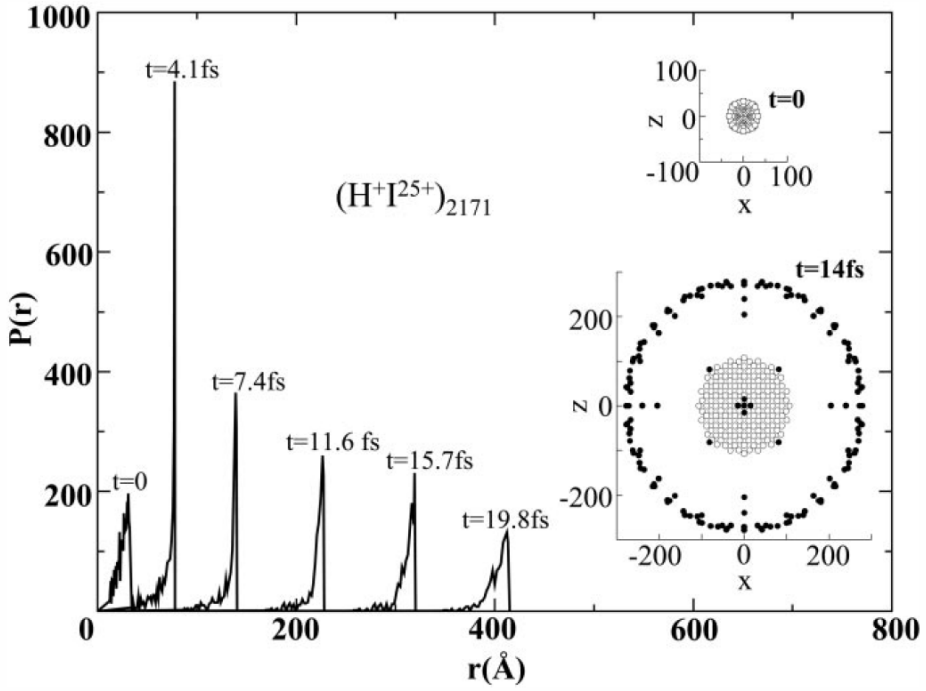

MD simulation of Coulomb explosion of $(H^+I^{25+})_{2171}$, narrow radial distribution of H^+ ions. In insets open circles I^{25+} , black dots H^+. (I. Last, J. Jortner, PNAS **102** (2005) 1291)

Applications of particle-cluster technique

- **3D Simulations of Laser-Target Interactions**
  - Rare – small macroscopic target (P. Gibbon et al. – fs laser interaction with wire of 1 – 4 μm radius – Phys. Plasmas 11(2004) 4032)
  - Parallel **tree code** PEPC (Pretty Efficient Parallel Coulomb-solver)
  - Laser included via ponderomotive source term, phase matched to instantaneous critical surface + spatial variations (not self-consistent)

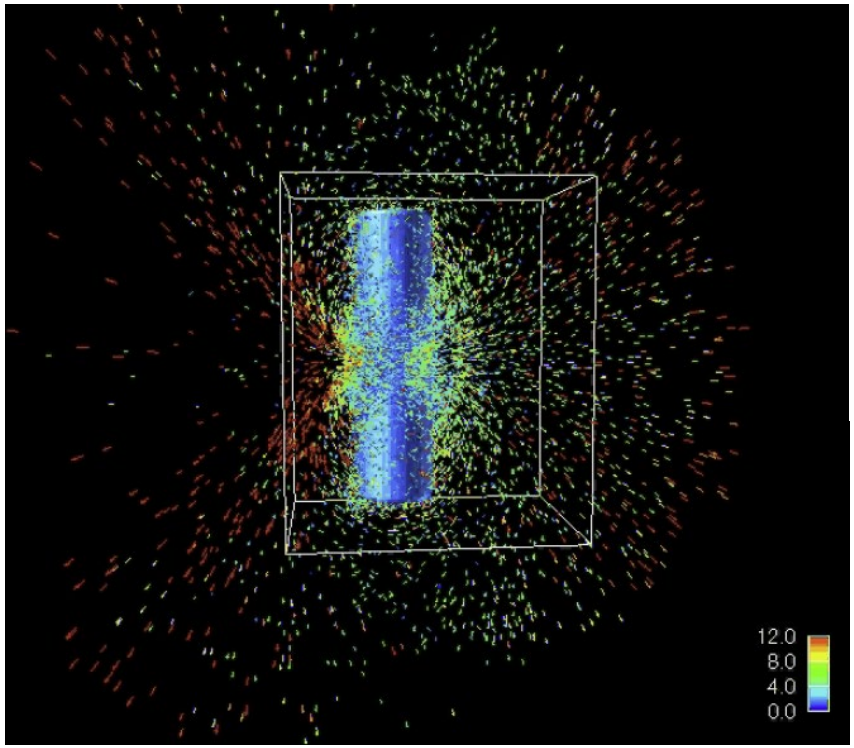

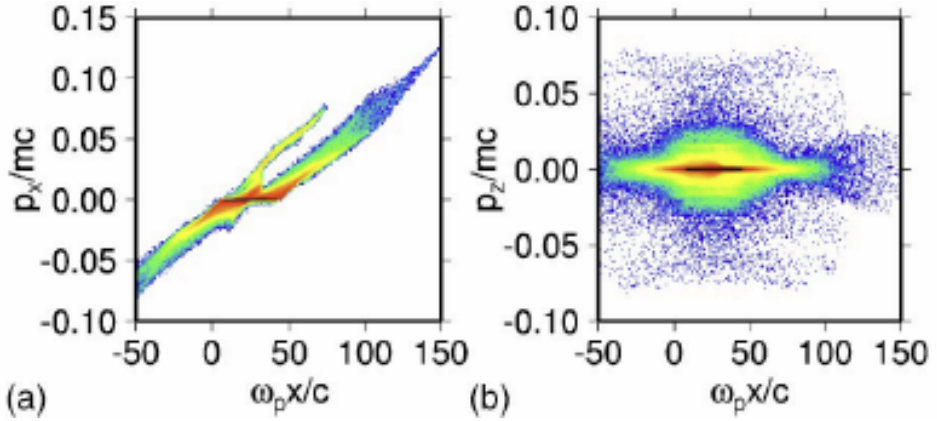

Electrons 50 fs after start of interaction of 2.5×10^{19} W/cm^2 laser with 4 μm wire (electron travel up to 30 μm from the wire (laser incident from the left)
Ion phase space at the end of run – x = laser direction (wire initially x = 0 – 50)

Molecular dynamics for microscopic processes

- **Collisional integrals** in kinetic eq. use Coulomb Logarithm
  - Approximately correct for weakly coupled plasmas
  - Incorrect for strongly coupled (kinetic energy < potential energy)
- **P^{3}M technique** (book by Hockney and Eastwood)
  - Point-like purely classical particles
  - **Collisions** (short-range particle interactions) are modelled accurately (often analytic two-body solution)
  - Long-range effects calculated by solving Poisson equation on a mesh
  - Periodic boundary conditions

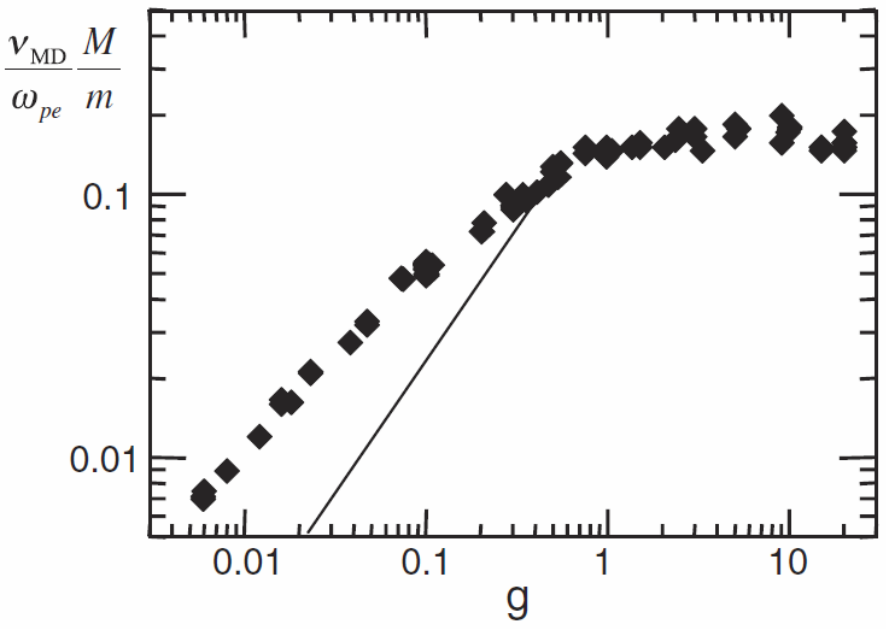

Electron-ion relaxation rate versus plasma parameter $g = Ze^2/\lambda_D k_B T_e$ (line – visual aid for constant Coulomb log)
(Dimonte, Daligault, PRL 101 (2008) 135001

Solution of equation for distribution function

- Vlasov equation
  - Computationally more demanding, originally 1D codes, but 2D simulations are also performed at present
  - Absence of noise, preferential when distribution tail matters or high noise leads to unphysical effects (pump depletion by noise)
  - Trend to formation of small scale structures in configuration space, small number of artificial collisions usually introduced

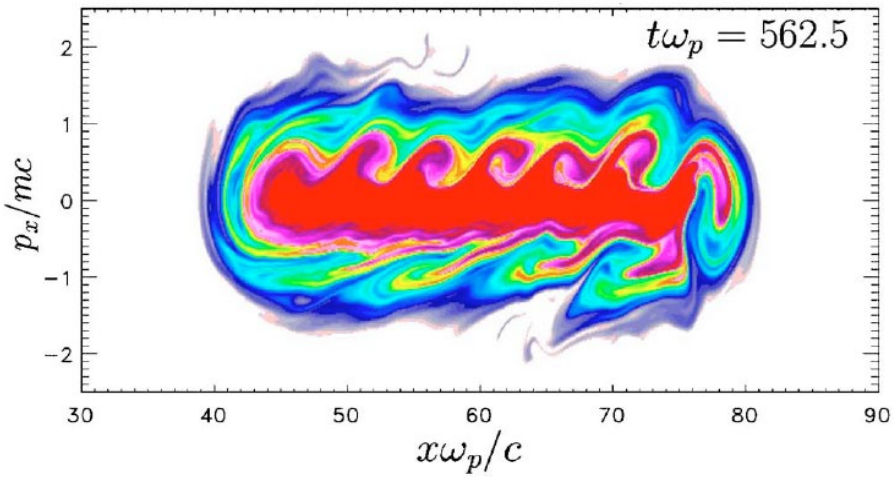

The phase space of relativistic KEEN wave in Vlasov simulations of stimulated Raman scattering (*A. Ghizzo et al., Phys. Rev. E* ***74*** *(2006), 046407*)

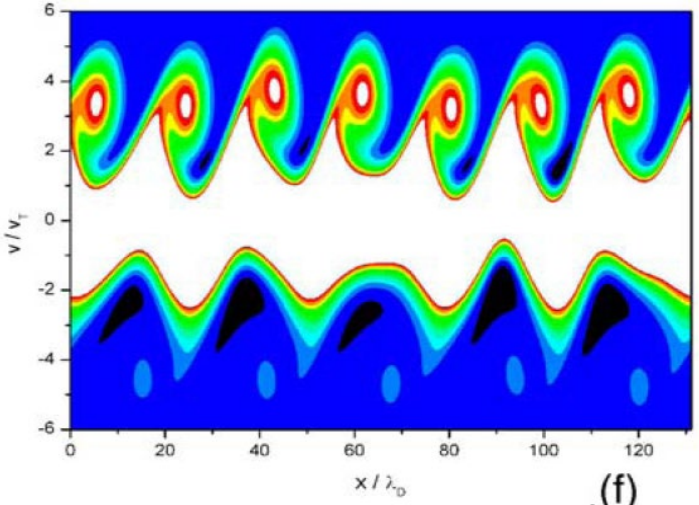

Phase-space contour plot of electron distribution function at time (f) $\omega_{pe}t$ = 1100. *(M. Masek, K. Rohlena, Eur. Phys. J. D (2009), 79-90.)*

Collisional kinetic equations

- Kinetic equations may use various collision terms – Fokker-Planck is the most frequent (Boltzmann; Lenard-Balescu)
- Overdense plasma between critical and ablation surface is usually highly collisional
- Studied effects (most frequently)
  - Non-local electron heat transport
  - Collisional (inverse bremstrahlung) laser absorption and its impact on electron distribution
  - Impact of atomic processes (ionization, excitation,…)
- Types of codes
  - Vlasov-Fokker-Planck codes – fields calculated from field equations (Poisson eq. or Maxwell's eqn.) – high frequency processes included
  - Quasineutral Fokker-Planck codes – electric field calculated from quasineutrality condition – only low frequency processes modelled

Fokker-Planck equation

$$\frac{\partial}{\partial t} f_a(\vec{r},\vec{p},t) + \vec{\mathrm{v}} \nabla_{\vec{r}} f_a(\vec{r},\vec{p},t) + \vec{F} \nabla_{\vec{p}} f_a(\vec{r},\vec{p},t) = \left(\frac{\partial f_a}{\partial t}\right)_c = \sum_b \left(\frac{\partial f_a}{\partial t}\right)_{cab}$$

where FP collisional term on the right hand side is

$$\left(\frac{\partial f_a}{\partial t}\right)_c = \frac{\partial}{\partial p_{ai}} \sum_b \frac{q_a^2 q_b^2}{8\pi\varepsilon_0^2} \ln\Lambda_{ab} \int \mathrm{d}\vec{p}_b \frac{\mathrm{v}_{ab}^2 \delta_{ij} - \mathrm{v}_{abi}\,\mathrm{v}_{abj}}{\mathrm{v}_{ab}^3} \left(\frac{\partial f_a}{\partial p_{aj}} f_b - f_a \frac{\partial f_b}{\partial p_{bj}}\right)$$

In non-relativistic case – velocity is usually used instead of momentum
Distribution function is often written as series of spherical harmonics in velocity (eigenfunctions of FP collision operator)

$$f(\vec{r},\vec{\mathrm{v}},t) = f_0(\vec{r},\mathrm{v},t) + \frac{\vec{\mathrm{v}}}{\mathrm{v}} \vec{f}_1(\vec{r},\mathrm{v},t) + \left(\frac{\mathrm{v}_i \mathrm{v}_j}{\mathrm{v}^2} - \frac{1}{3}\delta_{ij}\right) f_{2ij}(\vec{r},\mathrm{v},t) + \ldots.$$

In 1D case

$$f(x,\vec{\mathrm{v}},t) = \sum_{l=0}^{\infty} f_k(x,\mathrm{v},t)\, P_k(\mu), \quad \text{where } \mu = \mathrm{v}_x / \mathrm{v}$$

In the simplest case only 2 first terms

$$f(x,\vec{\mathrm{v}},t) = f_0(x,\mathrm{v},t) + \frac{\mathrm{v}_x}{\mathrm{v}} f_1(x,\mathrm{v},t)$$

Numerical scheme

- Discretization - method of alternating directions
- Inner points

$$\frac{f_{jk}^{0,n+1}-f_{jk}^{0n}}{h^t}+\frac{v_j}{3}\frac{f_{j,k+1/2}^{1,n+1}-f_{j,k-1/2}^{1,n+1}}{h_k^z}-\frac{a_k}{3v_j^2}\frac{f_{j+1/2,k}^{1n}v_{j+1/2}^2-f_{j-1/2,k}^{1n}v_{j-1/2}^2}{h_j^v}=$$
$$\frac{Y_k^{ee}}{v_j^2}\left(\frac{K_{j+1/2,k}^0 f_{j+1/2,k}^{0n}-K_{j-1/2,k}^0 f_{j-1/2,k}^{0n}}{h_j^v}+\right.$$
$$\left.\frac{1}{h_j^v}\left(K_{j+1/2,k}^1\frac{f_{j+1,k}^{0n}-f_{jk}^{0n}}{1/2\left(h_{j+1}^v+h_j^v\right)}-K_{j-1/2,k}^1\frac{f_{jk}^{0n}-f_{j-1,k}^{0n}}{1/2\left(h_{j-1}^v+h_j^v\right)}\right)\right)$$
$$v_j\frac{f_{j,k+1}^{0,n+1}-f_{jk}^{0,n+1}}{1/2\left(h_{k+1}^z+h_k^z\right)}-a_{k+1/2}\frac{f_{j+1,k+1/2}^{0n}-f_{j,k+1/2}^{0n}}{1/2\left(h_{j+1}^v+h_j^v\right)}=-\frac{Y_k^{ei}n_{k+1/2}^i}{v_j^3}f_{j,k+1/2}^{1,n+1}$$

$$\frac{f_{jk}^{0,n+2}-f_{jk}^{0,n+1}}{h^t}+\frac{v_j}{3}\frac{f_{j,k+1/2}^{1,n+1}-f_{j,k-1/2}^{1,n+1}}{h_k^z}-\frac{a_k}{3v_j^2}\frac{f_{j-1/2,k}^{1,n+2}v_{j-1/2}^2-f_{j+1/2,k}^{1,n+2}v_{j+1/2}^2}{h_j^v}=$$
$$\frac{Y_k^{ee}}{v_j^2}\left(\frac{K_{j+1/2,k}^0 f_{j+1/2,k}^{0,n+2}-K_{j-1/2,k}^0 f_{j-1/2,k}^{0,n+2}}{h_j^v}+\right. \qquad (4.55)$$
$$\left.\frac{1}{h_j^v}\left(K_{j+1/2,k}^1\frac{f_{j+1,k}^{0,n+2}-f_{jk}^{0,n+2}}{1/2\left(h_{j+1}^v+h_j^v\right)}-K_{j-1/2,k}^1\frac{f_{jk}^{0,n+2}-f_{j-1,k}^{0,n+2}}{1/2\left(h_{j-1}^v+h_j^v\right)}\right)\right)$$
$$v_{j+1/2}\frac{f_{j+1/2,k+1/2}^{0,n+1}-f_{j+1/2,k-1/2}^{0,n+1}}{h_k^z}-a_k\frac{f_{j+1,k}^{0,n+2}-f_{jk}^{0,n+2}}{1/2\left(h_{j+1}^v+h_j^v\right)}=-\frac{Y_k^{ei}n_k^i}{v_{j+1/2}^3}f_{j+1/2,k}^{1,n+2}$$

plus spatial and velocity boundaries plus edges

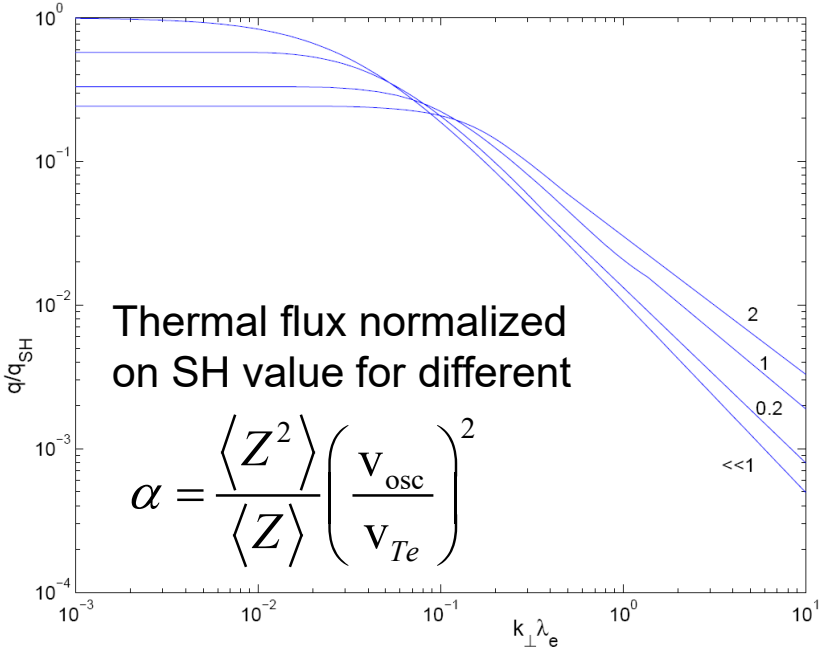

Thermal flux normalized on SH value for different

$$\alpha = \frac{\langle Z^2 \rangle}{\langle Z \rangle} \left(\frac{\mathrm{v}_{\mathrm{osc}}}{\mathrm{v}_{Te}} \right)^2$$

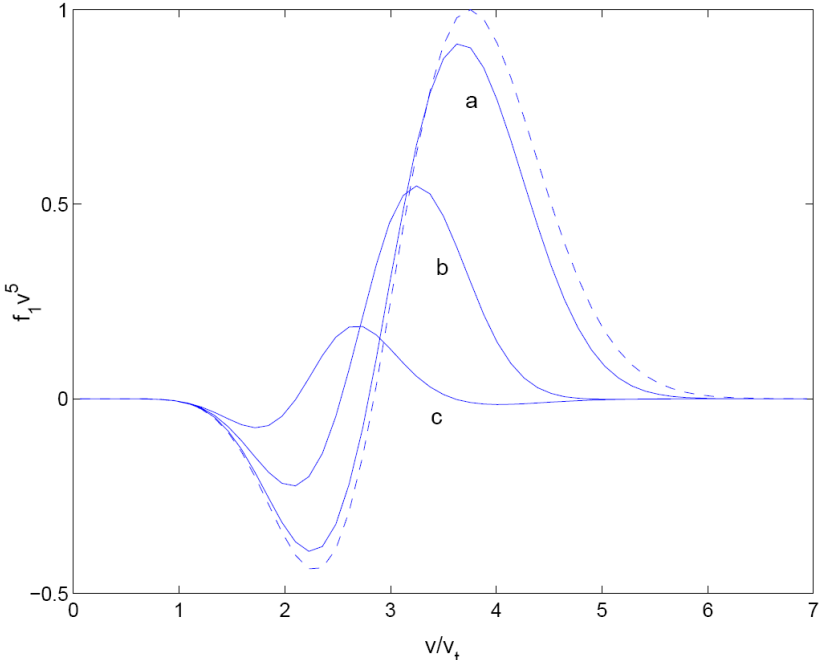

(a) $k_\perp \lambda_e = 0.01$; (b) $k_\perp \lambda_e = 0.05$; (c) $k_\perp \lambda_e = 0.2$

dotted – Spitzer-Harm (SH)

λ_e – electron mean free path
$k_\perp = 2\pi/L_T$ (L_T–temp. scale length)

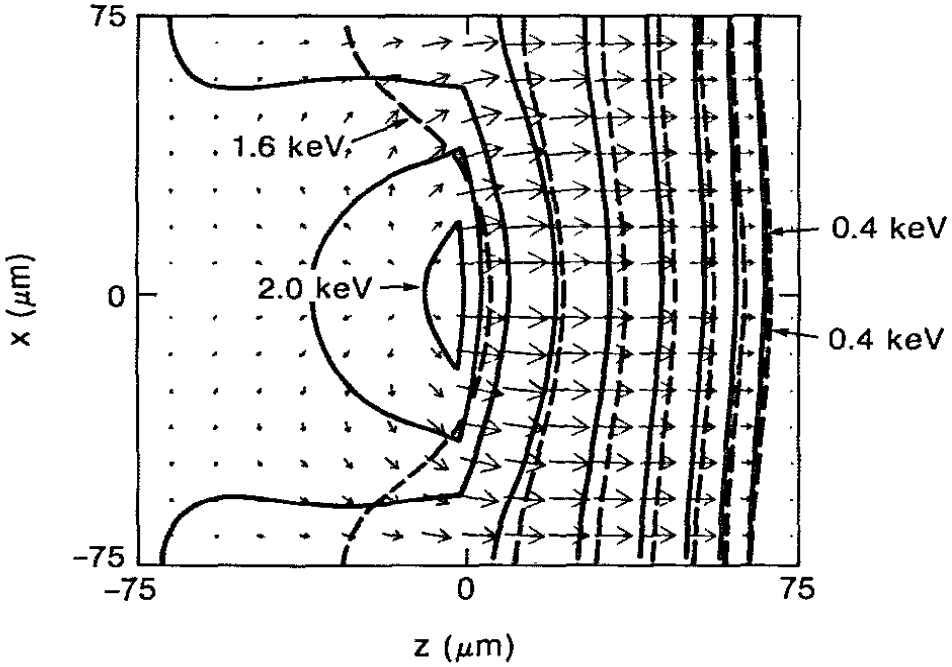

2D Fokker-Planck simulation of target heating by nonuniform laser irradiation

Fluid description

- Variables are moments of the distribution function
- Density $n_a = \int f_a(\vec{r}, \vec{\mathrm{v}}, \mathrm{t})\, \mathrm{d}\vec{\mathrm{v}}$
- Average velocity $\vec{w}_a = \frac{1}{n_a} \int f_a \vec{\mathrm{v}}\, \mathrm{d}\vec{\mathrm{v}}$
- Thermal (internal) energy $\varepsilon_{ka} = \frac{m_a}{2} \int f_a\, (\mathrm{v} - \vec{w}_a)^2\, \mathrm{d}\vec{\mathrm{v}}$
- PDE in $(\vec{r}, t)$, not in $\vec{\mathrm{v}}$
- Less computationally demanding, preferred for strongly collisional systems where distribution is near to equilibrium
- It needs equation of state $p_a = p_a(n_a, T_a), \varepsilon_a = \varepsilon_a(n_a, T_a)$; for single fluid description mass density ρ is used
- It can treat any state of matter, it enables including dense cold regions into simulations

Fluid description

- Fluid equations describe conservation of particle number (mass), momentum and energy
- Two (electron and ion) fluid equations are rarely used due to short timescale (ω_p^{-1}) and fast non-linearities (PIC preferred)
- One fluid equations may be used due to quasi-neutrality (consequently fast ~ ω_p^{-1} processes are omitted)
- Two (electron and ion) temperatures are often assumed as electron-ion energy relaxation is slow
- Radiation hydrodynamics is applied for higher Z targets as radiation transfer of energy is important
- Magnetohydrodynamics is used when imposed and/or self-induced magnetic fields are important
- When dissipative processes (thermal conduction, viscosity etc.) are omitted, fluid is described by Euler equations

Euler equations

- Euler equations = conservation laws for mass, vector of momentum and energy (hyperbolic PDE system)

$$\frac{\partial \rho}{\partial t} + \operatorname{div}\left(\rho \vec{w}\right) = 0$$

$$\frac{\partial \left(\rho \vec{w}\right)}{\partial t} + \operatorname{div}\left(\rho \vec{w} \vec{w}\right) + \operatorname{grad} p = 0$$

$$\frac{\partial E}{\partial t} + \operatorname{div}\left[\vec{w}\left(E + p\right)\right] = 0$$

- Here ρ is mass density, *w* is velocity vector, *p* is pressure and *E* is total energy density expressed via internal energy density ε ($\varepsilon = E/\rho - \left|\vec{w}\right|^2/2$).
- EoS connects p, ε with ρ, T. It also calculates mean ion charge $\overline{Z}$. The simplest EoS is ideal gas, for more realistic simulations either simplified analytic EoS (QEOS, Badger) are used or tabular EoS (SESAME) is interpolated (consistency?!)

Additional terms

- Laser absorption
  - Stationary approximation is often used
  - Ray tracing algorithm can follow propagation in underdense plasma (straight propagation inside cells, Snell's law at the cell boundaries)
  - Collisional (inverse bremsstrahlung) absorption in underdense plasma
  - Reflection and absorption in the critical surface vicinity (hydrodynamic grid usually does not resolve wavelength $\rightarrow$ interpolation, approximation)
  - Nonlinear effects (parametric instabilities etc.) may be taken into account in phenomenological way only
- Electron-ion relaxation
  - Energy per unit mass gained per unit time by ions from electrons is

$$Q_{ei} = G\left(T_e - T_i\right) = \frac{1}{\tau_i}\frac{d\varepsilon_i}{dT_i}\left(T_e - T_i\right) = \frac{3m_e k_B \nu_{ei}}{m_i^2}\left(T_e - T_i\right)$$

where ion specific heat $d\varepsilon_i/dT_i = 3k_B/(2m_i)$ in ideal gas state and characteristic time for ion heating is $\tau_i = m_i/(2m_e \nu_{ei})$.

$\nu_{ei} = \dfrac{4\sqrt{2\pi}\,\bar{Z}^2 e^4 n_i}{3\sqrt{m_e}\left(4\pi\varepsilon_0\right)^2\left(k_B T_e\right)^{3/2}}\ln\Lambda_{ei}$, where $\bar{Z}$ is mean ion charge and ln Λ_{ei} is Coulomb logarithm

Additional terms - continued

- Heat conduction
  - Ion heat flux usually << electron heat flux
  - Classical Spitzer-Harm electron heat-flux

$$\vec{Q}_e = -\frac{\xi_0 n_e k_B^2 T_e}{m_e \nu_{ei}} \nabla T_e = -\kappa_0 T_e^{5/2} \nabla T_e$$

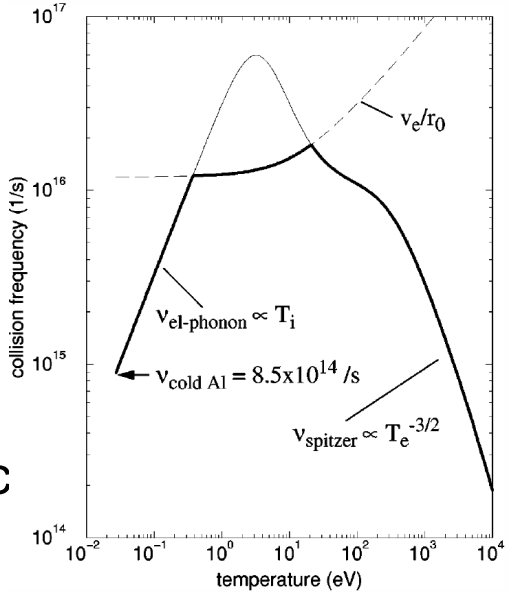

  - Heat conductivity derived for ideal plasma, one can modify collision frequency to obtain realistic heat flux in cold dense areas (Eidman, PRE 2000)
  - Electric field is self-induced to eliminate particle flux (return current)
  - Classical heat conduction is first order perturbation term, it is accurate, when $L_T/L_{mfp} \geq 200$ (due to $L_{mfp} \sim v^4$)
  - Temperature gradients are large in laser-target interactions, flux limited heat conduction is often used [$Q_{lim} = \min(Q_e, f \times Q_{free})$; $f \sim 0.03 - 0.1$]
  - Flux limitation is crude incorrect approximation, heat flux is **non-local**; some kind of **convolution** is needed to express non-local heat flux, problems in multi-dimensions; SNB model (Schurtz et al. 2000) introduced analytical solution of BGK kinetic equation and derived suitable form of closure for expression of non-local heat flux for fluid codes

Radiative transport

- Radiation transport plays essential role for high-Z targets
- Radiation transport is described by equation

$$\underbrace{\frac{1}{c}\frac{\partial I_\nu}{\partial t}}_{\approx 0} + \vec{n}\cdot\nabla I_\nu = j_\nu + \sigma_{s\nu}\bar{I}_\nu - \left(k_\nu' + \sigma_{s\nu}\right) I_\nu$$

  where $I_\nu\left(t,\vec{r},\vec{n}\right)$ is the radiation spectral intensity, angular averaged spectral intensity $\bar{I}_\nu = \int I_\nu \,\mathrm{d}\vec{n}/(4\pi)$, k_ν' is the opacity (including stimulated emission), $\sigma_{s\nu}$ is scattering coefficient and the emissivity $j_\nu = k_\nu' I_{\nu p}$
- Energy density $U_\nu = 4\pi\bar{I}_\nu / c$ and energy flux $\vec{S}_\nu = \int \vec{n}\, I_\nu \,\mathrm{d}\vec{n}$
- Radiation transport is solved in multi-group approximation or more simply in one-group (grey) approximation
- Diffusion approximation $\mathrm{div}\,\vec{S}_\nu = ck_\nu'\left(U_{\nu p} - U_\nu\right) \qquad k_\nu'\vec{S}_\nu = -c\nabla U_\nu / 3$
- Transport is diffusive in dense cold target, but is near to free streaming in hot corona (non-local radiative transport)

Types of computational meshes

- **Eulerian methods**
  - Numerical methods for solving fluid equations on a static computational mesh
  - Fluid moves through the computational mesh in form of mass fluxes
  - **Advantages** – typically simple (easy to implement) methods; well understood mathematical theory analyzing their accuracy and numerical stability; similar for all physical quantities
  - **Disadvantages** – not suitable for tasks with significant expansions or compressions in the computational domain; difficult simulation of fluid-vacuum boundary

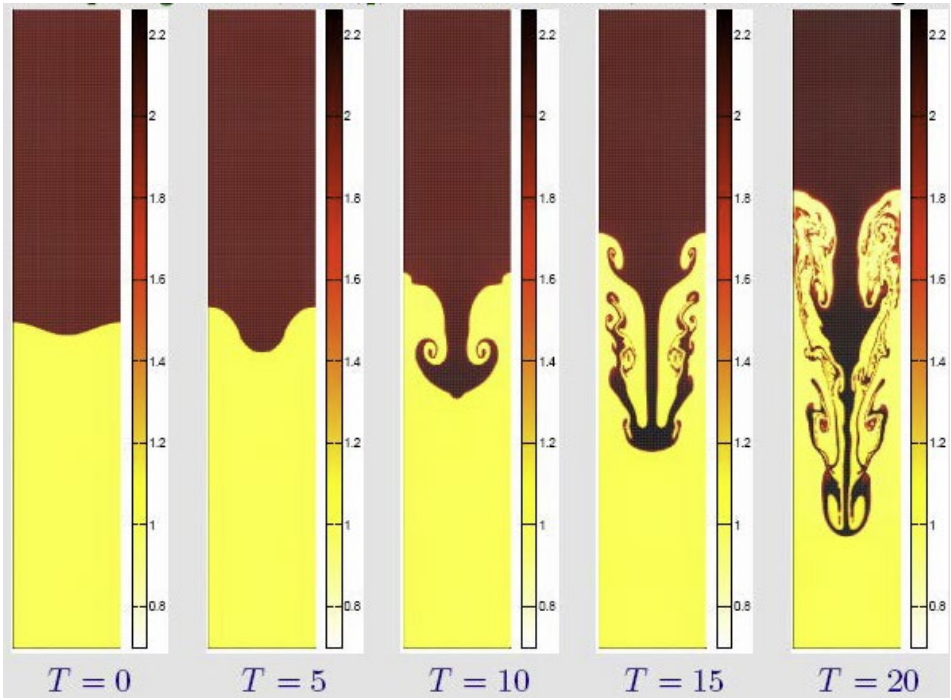

Numerical example – Rayleigh-Taylor instability (Fung et al. 2006), 100×600 Eulerian mesh

Problems of fluid simulations

Eulerian simulations cannot include **vacuum** – gas with density << critical density, but >> density in chamber

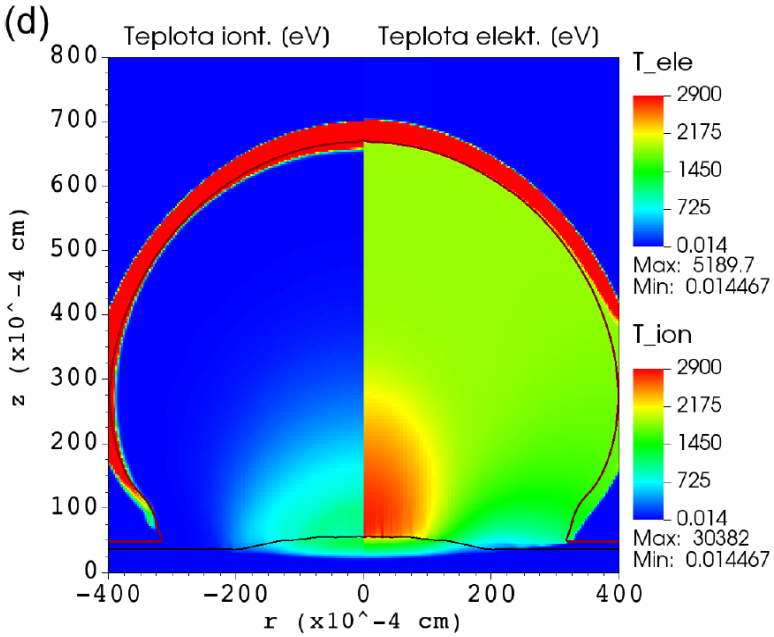

Expanding plasma launches **shock wave** into gas – unphysical high temp at plasma/gas boundary ($T_i \approx 30$ keV, $T_e \approx 5.2$ keV), **FLASH** code, He density 10^{-8} g/cm^3, Al target 30 μm thick, t = 400 ps

Ray-tracing algorithms of laser propagation often lead to numerical filamentation of laser beam

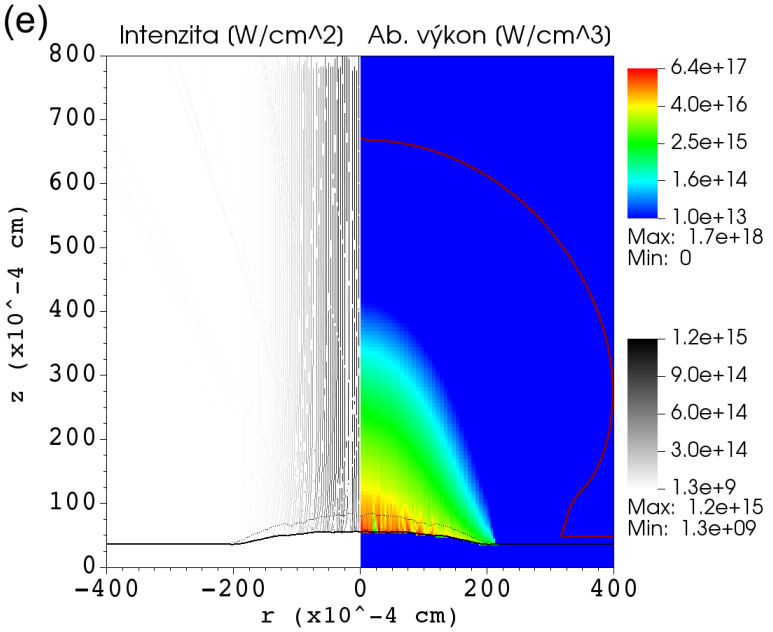

Right – absorbed energy distribution, left – ray trajectories + laser intensity
Time 400 ps (laser maximum), max. intensity 1.2×10^{15} W/cm^2, λ = 439 nm, Gaussian pulse FWHM length 400 ps, FWHM width 100 μm (Gaussian)

Lagrangian formulation

- **Lagrangian coordinates** are attached to the fluid and moving with it
  - Mass is constant in each cell, no mass fluxes through cell boundaries
  - Motion of node *n* is defined by $\dot{\vec{r}}_n = \vec{w}_n$
  - One fluid two-temperature equations in Lagrangian formulation

$$\frac{\mathrm{d}\rho}{\mathrm{d}t} = -\rho \nabla \vec{w}$$

$$\rho \frac{\mathrm{d}\vec{w}}{\mathrm{d}t} = -\nabla\left(p_i + p_e\right) + \vec{f}_V$$

$$\rho \frac{\mathrm{d}\varepsilon_\mathrm{i}}{\mathrm{d}t} = -p_i \nabla \cdot \vec{w} - G\left(T_i - T_e\right) - \nabla \cdot \vec{Q}_i$$

$$\rho \frac{\mathrm{d}\varepsilon_\mathrm{e}}{\mathrm{d}t} + \frac{\mathrm{d}\varepsilon_\mathrm{R}}{\mathrm{d}t} = -p_e \nabla \cdot \vec{w} + G\left(T_i - T_e\right) - \nabla \cdot \left(\vec{Q}_e + \vec{Q}_R + \vec{Q}_L\right)$$

where p_e, p_i are electron and ion pressures, ε_e, ε_i are electron and ion specific internal energies, f_V is volume force, ε_R is radiation energy density, G is coffient of electron-ion energy relaxation, Q_e, Q_i, Q_R, Q_L are energy/heat fluxes of electrons, ions, radiation and laser field

- **Advantages** – moving mesh naturally follows the fluid (including plasma-vacuum boundary), suitable for severe expansions or compressions
- **Disadvatages** – mesh can tangle (leading to errors and method failure)

Lagrangian fluid simulation result
(interaction of subnanosecond pulse with foil)

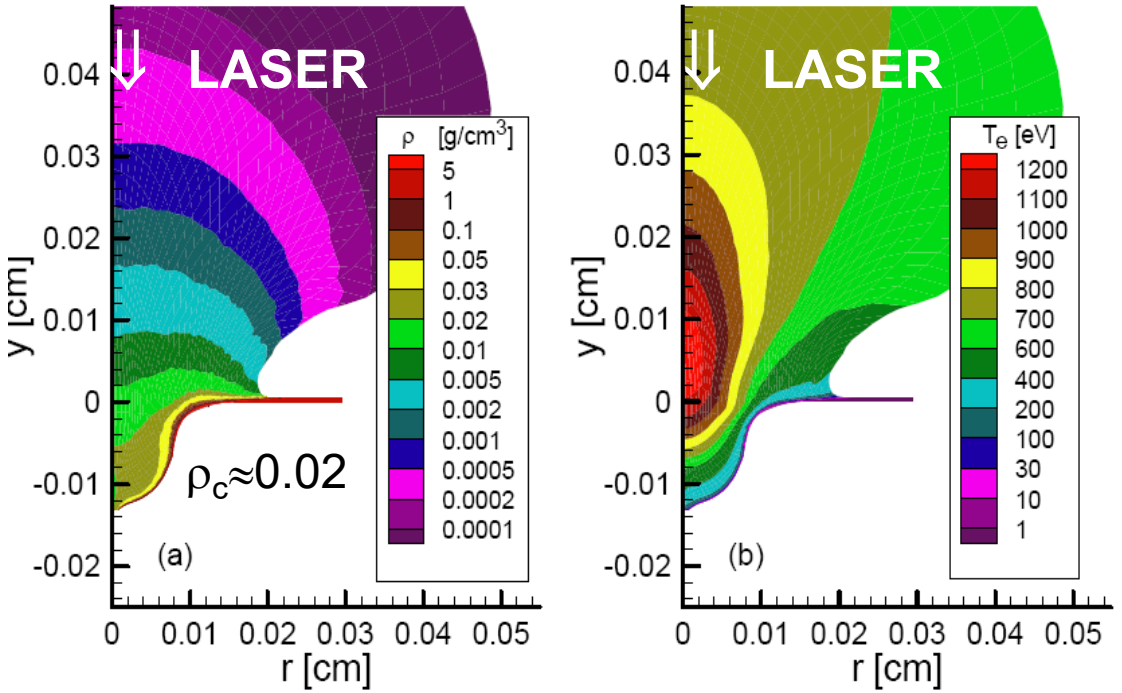

*O. Renner, J. Limpouch et al., JQSRT **81** (2003), 385-394.*

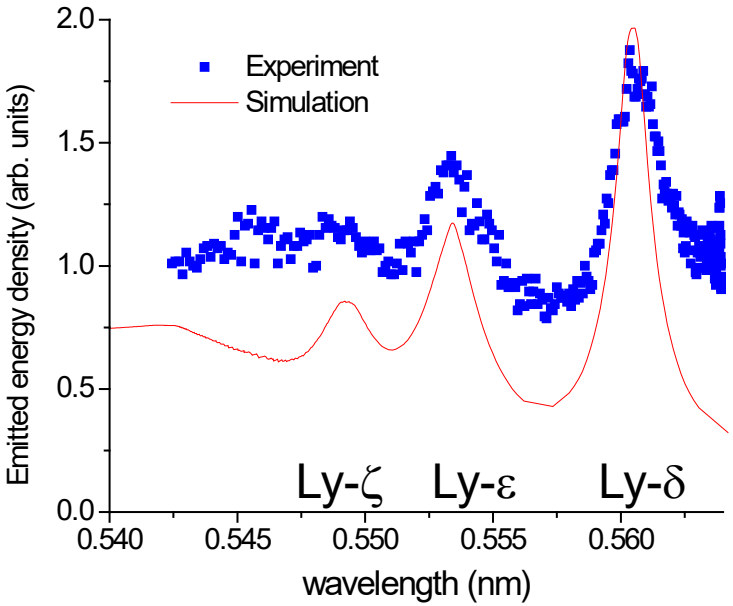

(a) Density profile, (b) Temperature profile – in time of maximum emission of studied lines - 300 ps after 400-ps laser pulse maximum. 2D Lagrangian fluid simulation in cylindrical geometry. Laser beam λ = 0.439 μm (3ω) of radius 40 μm normally incident on 5 μm-thick Al foil, laser energy 58 J, I_{max}= 3×10^{15} W/cm^2

Time-integrated spectrum in region of lines of H-like Al emitted 50 μm behind original foil position tangentially to the s foil – measurement VJS and post-processor XEPAP

Arbitrary Lagrangian-Eulerian (ALE) Method

- **Combination of Eulerian and Lagrangian approaches**
  1. **Lagrangian computation** of several time steps
  2. **Rezoning** – mesh untangling and improvement
  3. **Remapping** – conservative interpolation of the conservative quantities to the new, better mesh
  - 2. and 3. correspond to the Eulerian part

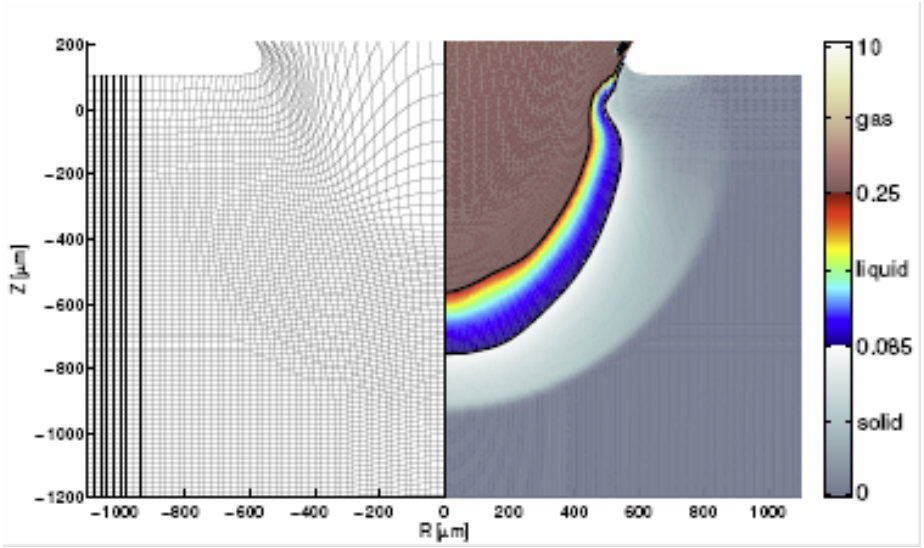

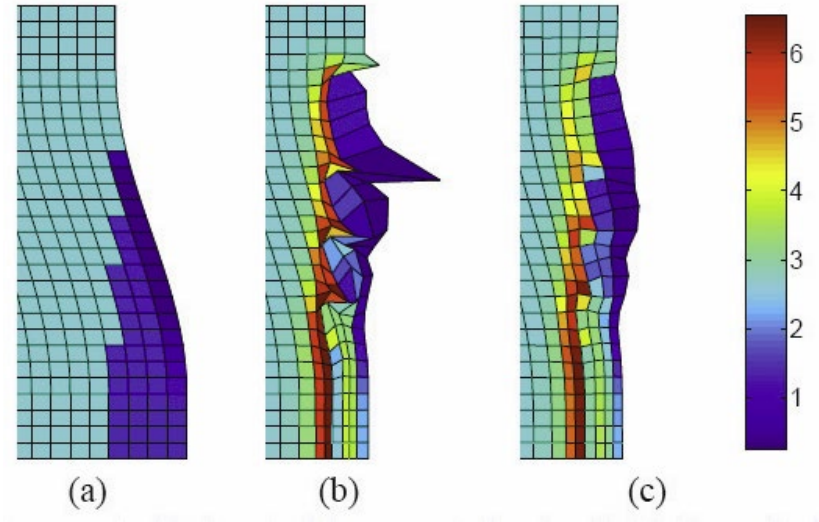

Numerical example – **PALE code** - Flyer-target impact – left panel – computational mesh and temperature contours (shock wave, phase interfaces) at 80 ns; right panel – density colormap of the critical part of the computational grid (a) initial grid before computation (b) very distorted Lagrangian grid at 0.5 ns includes non-convex cells (c) ALE grid is still fine at the end (80 ns) of computation

Magnetohydrodynamics

- Equation for quasi-static magnetic field (extended MHD)

$$\frac{\partial \vec{B}}{\partial t} = -\nabla \times \frac{\alpha_{\parallel}}{\mu_0 e^2 n_e^2} \nabla \times \vec{B} + \nabla \left(\vec{v}_B \times \vec{B} \right) + \nabla \times \frac{\nabla \overleftrightarrow{P_e}}{e n_e}$$

Here, the last term is the Biermann battery source term of magnetic field, the first term is magnetic field diffusion and the second term is magnetic field convection with advection velocity

$$\vec{v}_B = \vec{v} - \gamma_{\perp} \nabla T_e - \gamma_{\wedge} \left(\vec{b} \times \nabla T_e \right) - \frac{\vec{j}}{e n_e} \left(1 + \delta_{\perp}^c \right) + \frac{\delta_{\wedge}^c}{e n_e} \left(\vec{j} \times \vec{b} \right)$$

- Biermann battery term is key source for laser targets (not placed in external B)
- Proper discretization of Biermann battery term is difficult and many astrophysical codes do not include it
- Classical Braginski transport coefficients (1965) were improved by EH (1996), fitting of cross-Hall $\delta_{\wedge}$ and cross-Nernst $\gamma_{\wedge}$ erroneous at low magnetization $\chi = \omega_{ce} \tau_{ei}$ (Sadler 2021)

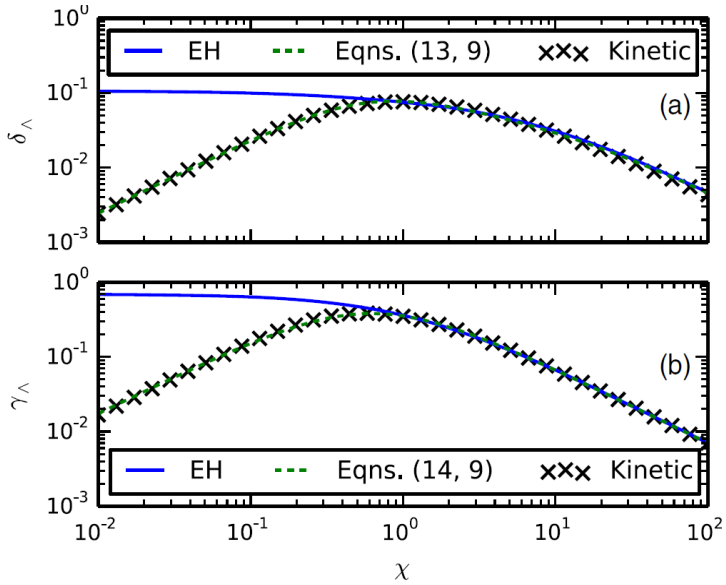

Magnetohydrodynamics -applications

- Laboratory astrophysics
  - recently demonstrated dynamo amplification in turbulent plasma (Tzerefacos et al., Nature Comms 2018)

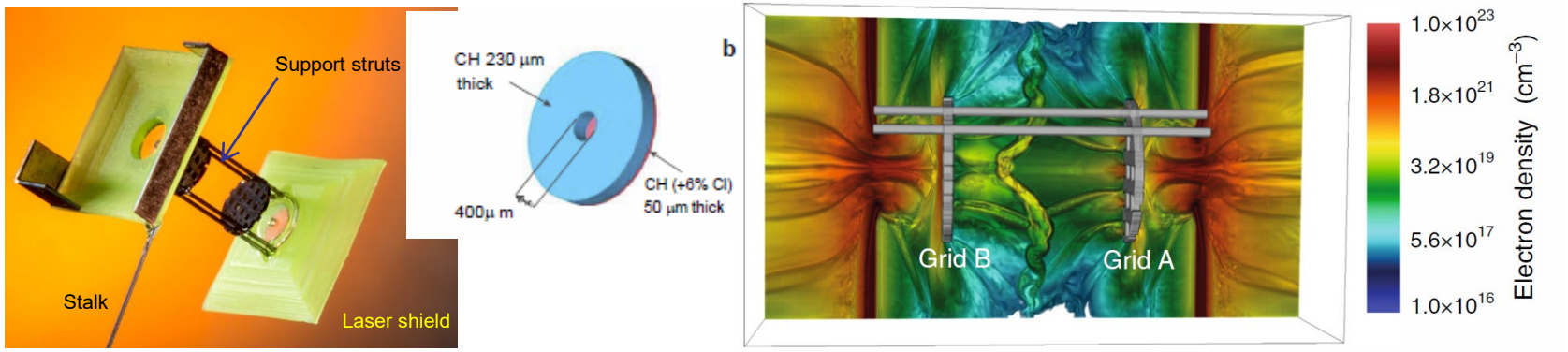

Laser beams are incident on targets (middle panel) placed into laser shields. Accelerated plasmas penetrate through grids and collide in the middle. Density calculated by 3D magnetohydrodynamic code FLASH (right)

  - Magnetic field in early phase of collision $\leq$ 4 kG, consistent with Biermann battery source (it does not grow for one-side irradiation)
  - Magnetic field is amplified to 100 -120 kG during collision
  - Magnetic Reynolds number ~600 reached (above dynamo threshold)
- Self-induced magnetic fields studied for ICF (Lancia. PRL 2014)
- Special targets

Capacitor- coil target

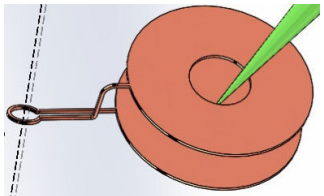

Snail (escargot) target

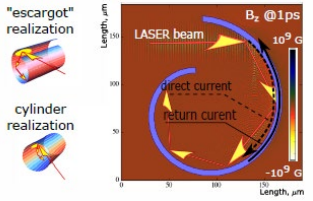

Hybrid models

- Hybrid means that different types of particles are modelled in different way
  - In astrophysics often ions are treated as particles and electrons as mass conduction fluid
  - In ultra-intense laser interactions – electrons accelerated by laser to high energies propagate into target and return current is induced to sustain quasi-neutrality
  - Hybrid simulations – particle simulation is run for fast electrons and the rest is modeled as conducting fluid ($\vec{E} = \vec{j}_b / \sigma$, where j_b is background return current and σ is electrical conductivity at background T_b). Background current is expressed from fast electron current j_f and B

$$\vec{j}_b = -\vec{j}_f + \nabla \times \vec{B} / \mu_0; \quad \partial \vec{B} / \partial t = -\nabla \times \vec{E}$$

- Interpretation of fast electron diagnostics and electron fast ignition studies

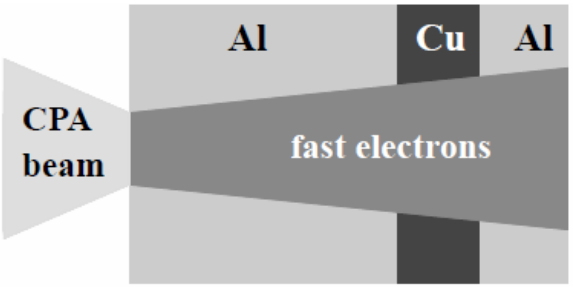

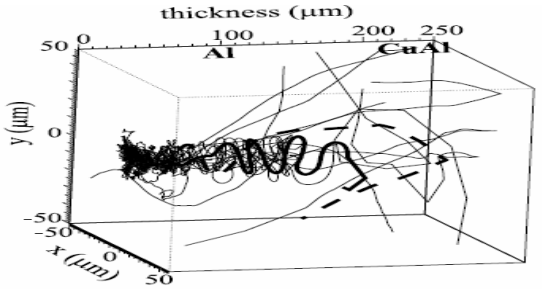

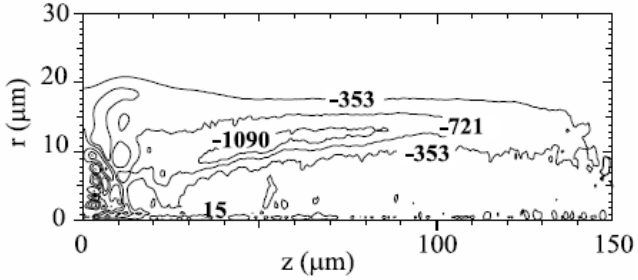

Typical simulation setup; fast electron trajectories; azimuthal magnetic field (T) (Honrubia, LPB 2004)

Summary

- Extremely broad range of simulation types is used for laser plasma interaction physics
- Main types of plasma dynamic simulations are
  - **Kinetic models** - simulate detailed non-linear physics of interaction, but cannot treat global evolution of dense targets,
    kinetic models are subdivided to
    - **Particle models**
    - **Solution of kinetic equations**
  - **Fluid models** – more simple, can treat solid targets globally, but interaction physics is described only phenomenologically

Thank you for attention